

# An electrochromic device (ECD) cell characterization on electron beam evaporated MoO<sub>3</sub> films by intercalating/deintercalating the H<sup>+</sup> ions

R. Sivakumar<sup>a</sup>, C.S. Gopinath<sup>b</sup>, M. Jayachandran<sup>c</sup>, C. Sanjeeviraja<sup>a,\*</sup>

<sup>a</sup> Department of Physics, Alagappa University, Karaikudi 630 003, India

<sup>b</sup> Catalysis Division, National Chemical Laboratory, Pune 411 008, India

<sup>c</sup> ECMS Division, Central Electrochemical Research Institute, Karaikudi 630 006, India

Received 19 October 2005; received in revised form 27 October 2005; accepted 5 December 2005

Available online 10 March 2006

## Abstract

Thin films of molybdenum oxide (MoO<sub>3</sub>) is one of the most interesting layered intercalation materials because of its excellent application in solid state batteries, large-area window and display systems. In recent years there has been considerable interest in variable transmittance electrochromic devices (ECD) based on Li<sup>+</sup>, H<sup>+</sup> and K<sup>+</sup> intercalation in transition metal oxide (MoO<sub>3</sub>) thin films. In the present investigation, thin films of MoO<sub>3</sub> were prepared by electron beam evaporation technique on microscopic glass and fluorine doped tin oxide (FTO) coated glass substrates for the application in electrochromic device cells. The compositional stoichiometry of the films was studied by X-ray photoelectron spectroscopy (XPS). The electrochromic nature of the films has been analyzed by inserting H<sup>+</sup> ions from the H<sub>2</sub>SO<sub>4</sub> electrolyte solution using the cyclic-voltammetry (CV) technique. We studied the electrochromic device cells (ECD) incorporating an evaporated MoO<sub>3</sub> thin films as electrochromic layers. The devices exhibit good optical properties with low transmittance values in the colored state, which make them suitable for large-area window applications. The maximum coloration efficiency of the cell was observed at about 70 cm<sup>2</sup>/C.

© 2005 Published by Elsevier B.V.

PACS: 64.70.F; 68.60; 68.55; 82.80; 42.80

Keywords: Molybdenum oxide thin films; Electrochromic device cells; Stoichiometry; Coloration efficiency; Optical density

## 1. Introduction

Electrochromism has been attracting a sustained interest for the past two decades. Electrochromism means to color by electricity and this property can be found among several organic and inorganic compounds [1,2]. Inorganic transition metal oxides exhibit electrochromism and can quite easily be deposited as thin films. The electrochromic material needs to be incorporated with supportive components,

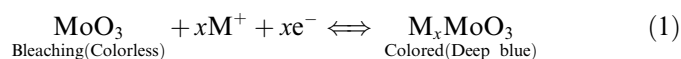
such as transparent electrical contacts and an ion conducting electrolyte, to provide electric currents. The electrochromic materials can be used in smart windows to modulate the transmission of solar radiation; in car mirrors to prevent glare during night driving; and, in information displays.

Thin film of molybdenum oxide (MoO<sub>3</sub>) is one of the transition metal oxides which has received much attention in recent years due to its important technological applications, such as, smart windows, electrochromic devices, solid state microbatteries and display panels [1,2]. In recent years, orthorhombic molybdenum oxide ( $\alpha$ -MoO<sub>3</sub>) has become an important starting compound in making many advanced materials. Such derivatives have been widely used

\* Corresponding author. Tel.: +91 4565 230 251; fax: +91 4565 230 251/225 202.

E-mail addresses: [krsivakumar1979@yahoo.com](mailto:krsivakumar1979@yahoo.com) (R. Sivakumar), [sanjeeviraja@rediffmail.com](mailto:sanjeeviraja@rediffmail.com) (C. Sanjeeviraja).

as charge-density wave conductors, optical materials, display devices, catalysis, intercalated materials for ion exchange and batteries [3]. The phenomenon of electrochromism was observed by the application of external potential between the working electrode and electrolyte containing cationic species  $M^+$  ions ( $M^+ = H^+, K^+$  and  $Li^+$ ) from the appropriate electrolyte solutions. The reduction in peak is associated with a deep coloration of the film and the bleaching process is marked by the oxidation peak. The coloration/bleaching process is reversible and governed by the double insertion/extraction of electrons and  $M^+$  ions and the typical molybdenum bronze is formed as follows [4]:



Before the electroreduction, the molybdenum oxide is a light grey in hue, all molybdenum sites having identical oxidation states of +IV. Reduction of  $\text{MoO}_3$  involves the electron transfer from an electrode  $\text{Mo}^{\text{VI}}$  (reduction) forms some  $\text{Mo}^{\text{V}}$  centres, and the desired blue for the electrochrome is produced. Partial reduction introducing negative charge requires charge compensation by cation insertion (say of  $M^+$ ), with a fractional insertion coefficient  $x$ , to form molybdenum ‘bronze’ ( $M_x\text{Mo}_x^{\text{V}}\text{Mo}_{(1-x)}^{\text{VI}}\text{O}_3$ ) (where  $M = \text{metal ion, i.e., } H^+, K^+, Li^+ \dots$ ) [2].

Electrochromic devices are of much interest in emerging technology, especially, in large-area smart windows, which are capable of varying the throughput of radiant energy under the action of voltage pulses [1,2]. Electrochromic glazings promise to be the next major advance in energy-efficient window technology, helping to achieve the goal of transforming windows and skylights from an energy liability in buildings to an energy source. The glazing can be reversibly switched from clear to a transparent, colored state by applying a low voltage, resulting in dynamically controllable thermal and optical properties (“smart windows”). The above processes can be achieved by attaching a suitable molecule that is colorless in the oxidized state and colored in the reduced state onto the surface of a colorless semiconducting electrochromic material (present case,  $\text{MoO}_3$ ) on conducting glass (present case, FTO substrates). When a sufficiently negative potential is applied, electrons are injected from the conducting glass into the conduction band of the semiconducting electrochromic material and reduce the absorbed molecules. The reverse process occurs when a positive potential is applied and the molecules get bleached.

However, different techniques have been used for the preparation of amorphous and crystalline electrochromic  $\text{MoO}_3$  films, such as sputtering [5], chemical vapor deposition [6], spray pyrolysis [7]. The considerable differences in deposition methods and conditions produce differences in structural, optical, morphological, as well as in the electrochemical properties. The microstructure and morphology play a significant role in the electrochromic intercalation and deintercalation process [2]. By controlling these

parameters, one could design a material with optimal electrochromic behaviour. This is an important factor in device applications. In respect of these requirements, the electron beam evaporation technique offers an excellent approach to the deposition of device oriented  $\text{MoO}_3$  coating optimized for commercial applications. In the present work the electrochromic  $\text{MoO}_3$  films have been prepared by electron beam evaporation technique. The detailed description for the preparation method of  $\text{MoO}_3$  films by electron beam evaporation technique was reported in our earlier work [8,9].

Indeed, the electrochemical analysis and electrochromic device performance of  $\text{MoO}_3$  films may depend on its structural nature, surface morphological behaviour, compositional stoichiometry and its optical performance. Hence, in order to explore the device performance of  $\text{MoO}_3$  films, the systematic characterization studies on structural, surface morphological and optical properties of electron beam evaporated  $\text{MoO}_3$  films have been studied and reported [8,9]. In the present investigation, we extend our studies to explore the compositional stoichiometry by X-ray photoelectron spectroscopy (XPS) and electrochemical analysis by cyclic voltammetry (CV). The CV studies were performed by intercalating/deintercalating the  $H^+$  ions from  $\text{H}_2\text{SO}_4$  electrolyte solutions. Shaoqin Liu et al. [10] reported the electrochromic behaviour of  $\text{MoO}_3$  films in  $\text{H}_2\text{SO}_4$  electrolyte solution. The cyclic voltammetry of  $\text{MoO}_3$  films in 0.3 M  $\text{LiClO}_4 \cdot \text{PC}$  electrolyte solution was studied by Gesheva et al. [6]. The electrochromic device performance of  $\text{MoO}_3$  films was also studied by constructing the three electrode electrochromic device (ECD) cells. The optical density (OD) and coloration efficiency (CE) of the films in ECD cells were also evaluated with respect to different substrate temperature and annealing temperature.

## 2. Experimental

The preparation of  $\text{MoO}_3$  thin films was carried out by using the electron beam evaporation technique on microscopic glass and fluorine doped tin oxide coated (FTO) ( $R_{\text{sh}} \sim 15 \Omega/\text{sq}$ ) glass substrates. The target was a compressed (palletized)  $\text{MoO}_3$  powder. These palletized  $\text{MoO}_3$  targets were taken in a graphite crucible and heated with  $180^\circ$  deflected resultant electron beam extracted from the tungsten filament with an accelerating voltage of 5 kV and power density of about  $1.5 \text{ kW}/\text{cm}^2$ . The evaporation was carried out in a pressure of about  $1 \times 10^{-5}$  mbar. The most homogeneous distribution of  $\text{MoO}_3$  particles on the substrate was gained by rotating the substrate holder during the deposition. The depositions were carried out at room temperature ( $30^\circ \text{C}$ , RT),  $100^\circ \text{C}$  and  $200^\circ \text{C}$ . The room temperature prepared films were further annealed at  $200^\circ \text{C}$  and  $300^\circ \text{C}$  for about one hour in vacuum environment.

The X-ray photoelectron spectroscopy (XPS) studies were carried out by a VG Microtech Multilab ESCA

3000 spectrometer with non-monochromatized  $\text{MgK}\alpha$  X-ray source ( $h\nu = 1253.6$  eV). The electrochemical behaviour of the films was analyzed by the cyclic-voltammetry technique using the EG&G Princeton applied research potentiostat/galvanostat model 273A with EG&G interface model 507. The analysis was performed in 0.05 M and 0.1 M  $\text{H}_2\text{SO}_4$  electrolyte solution. The optical transmission measurements were carried out by the Hitachi-3400 UV–Vis–NIR spectrometer in the wavelength range from 300 to 2500 nm.

### 3. Results and discussion

The electrochemical performance of  $\text{MoO}_3$  films can be mainly correlated with its structural and surface morphological properties. Hence, in order to explore the electrochromic device performance of  $\text{MoO}_3$  films, we have systematically studied and reported [8,9] the influence of substrate temperature and annealing temperature on structural and surface morphological properties of  $\text{MoO}_3$  films. The X-ray diffraction pattern of  $\text{MoO}_3$  films deposited at room temperature and 200 °C is shown in Fig. 1(a) and (b), respectively [9]. It resulted that the films deposited at

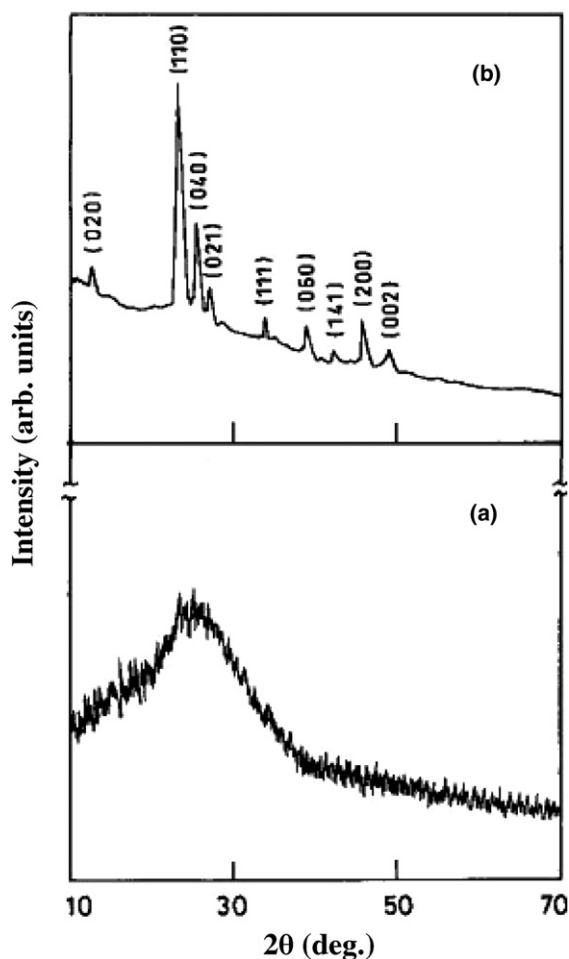
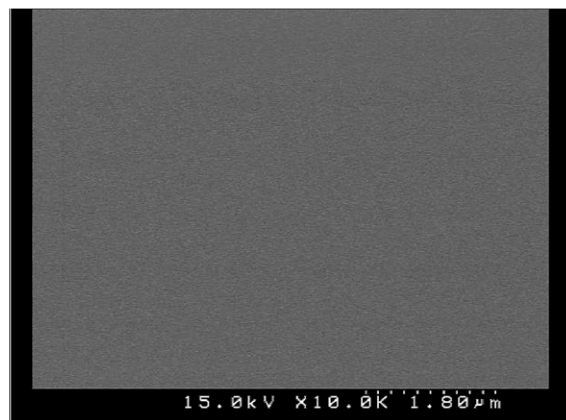
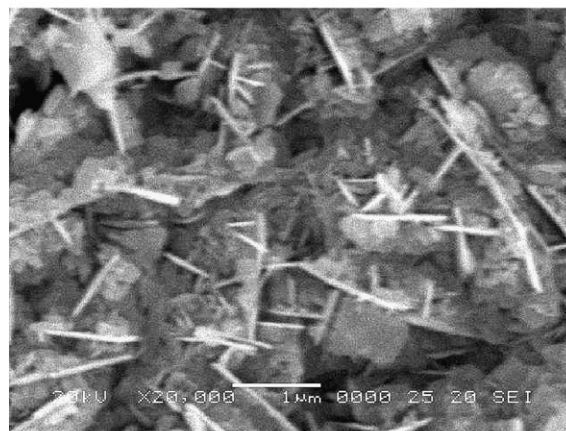


Fig. 1. X-ray diffraction pattern of  $\text{MoO}_3$  films on glass substrate at different substrate temperatures (a)  $T_{\text{sub}} = \text{RT}$ , (b)  $T_{\text{sub}} = 200$  °C.



(a)



(b)

Fig. 2. Surface morphology of  $\text{MoO}_3$  films on glass substrate at different substrate temperatures (a)  $T_{\text{sub}} = \text{RT}$ , (b)  $T_{\text{sub}} = 200$  °C.

room temperature belongs to the amorphous nature and the crystallinity of  $\text{MoO}_3$  films enhanced with increasing substrate temperature. The films deposited at 200 °C shows the crystalline nature, which clearly identified from the X-ray diffraction pattern (Fig. 1(b)). Fig. 2(a) and (b) shows the scanning electron microscopical images of  $\text{MoO}_3$  films deposited on glass at room temperature and 200 °C, respectively. This also confirmed the amorphous nature of the film prepared at room temperature (Fig. 2(a)) and it transformed into crystalline nature when the substrate was increased (Fig. 2(b)) [9] to 200 °C.

#### 3.1. Compositional analysis

In order to identify the compositional homogeneity, material quality and stoichiometric nature of  $\text{MoO}_3$  films, the compositional analysis was carried out by X-ray photoelectron spectroscopy. The survey scan information of this spectroscopic analysis is useful, particularly, in the identification of the elements present at the film surface. The XPS survey scan analysis of  $\text{MoO}_3$  films was carried out in the binding energy ( $E_b$ ) ranging between 0 and 1000 eV. All measurements were made on  $\text{MoO}_3$  films deposited on

glass substrates using  $MgK\alpha$  X-ray source. Base pressure in the analysis chamber was  $4 \times 10^{-10}$  Torr. Multichannel detection system with nine channels was used to collect the data. The overall energy resolution of the instrument is better than 0.7 eV. The errors in all the  $E_b$  values are within  $\pm 0.1$  eV.

Fig. 3(a)–(d) shows the X-ray photoelectron spectroscopy survey scan spectra of electron beam evaporated  $MoO_3$  films on glass substrates at conditioned  $T_{sub} = RT$ ,  $T_{sub} = 100^\circ C$ ,  $T_{sub} = 200^\circ C$  and  $T_{anne} = 300^\circ C$ , respectively. From the spectra, no peaks were observed other than the characteristic peaks of Mo and O, which infer the compositional purity and quality of  $MoO_3$  films. There are few reports [4,11,12] available for the X-ray photoelectron spectroscopic characterization on the  $MoO_3$  films. Based on these literatures, it can be said that the electrochromic mechanism of  $MoO_3$  films depends on the existence of different final states such as  $Mo^{6+}$  and  $Mo^{5+}$ . The core-level spectra of  $MoO_3$  films exhibit the characteristic Mo-3d<sub>5/2</sub> and Mo-3d<sub>3/2</sub> doublet caused by spin-orbit coupling [4]. The core-level spectra of molybdenum (Mo-3d) and oxygen (O-1s) for the  $MoO_3$  films are shown in

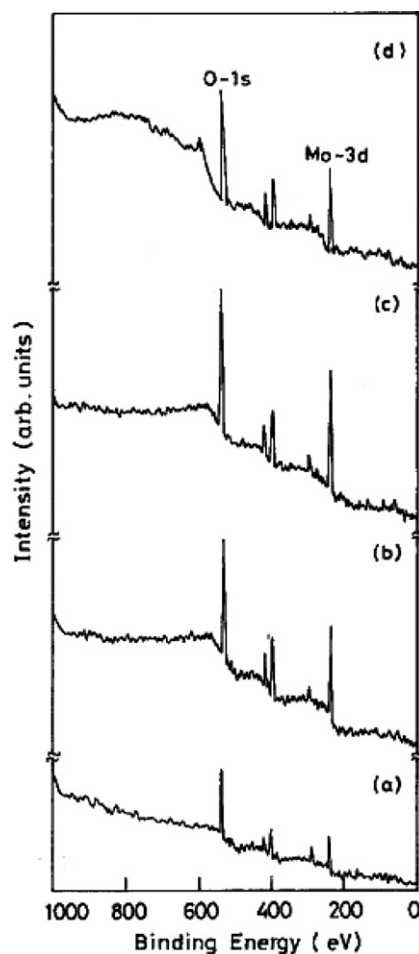


Fig. 3. X-ray photoelectron spectroscopy survey scan of  $MoO_3$  films on glass substrates at conditioned (a)  $T_{sub} = RT$ , (b)  $T_{sub} = 100^\circ C$ , (c)  $T_{sub} = 200^\circ C$  and (d)  $T_{anne} = 300^\circ C$ .

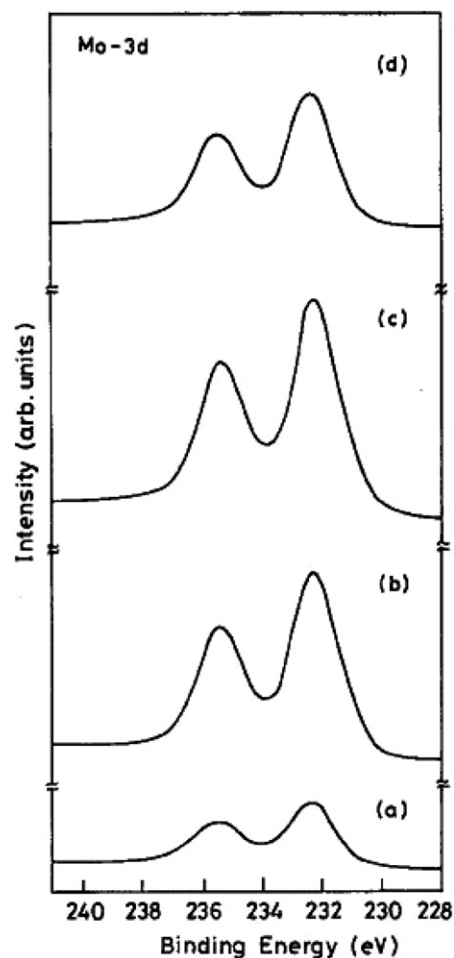


Fig. 4. XPS core-level spectra of molybdenum (Mo-3d) for  $MoO_3$  films (a)  $T_{sub} = RT$ , (b)  $T_{sub} = 100^\circ C$ , (c)  $T_{sub} = 200^\circ C$  and (d)  $T_{anne} = 300^\circ C$ .

Figs. 4(a)–(d) and 5(a)–(d), respectively. The characteristic doublet peaks are observed at binding energies of 232.32 and 235.44 eV from the Mo-3d core-level spectra (Fig. 4(a)–(d)). These doublet core-level binding energies i.e., 232.32 eV and 235.44 eV correspond to Mo-3d<sub>5/2</sub> and Mo-3d<sub>3/2</sub>, respectively, which are due to the spin-orbit splitting (Mo-3d) and are in good agreement with the values reported by the other workers for  $MoO_3$  films [4,13]. Hence, it reveals that the electron beam evaporated  $MoO_3$  films pertaining the six valence molybdenum ( $Mo^{6+}$ ). Julien et al. [12] also reported the core-level binding energies of Mo-3d<sub>5/2</sub> and Mo-3d<sub>3/2</sub> are 232.3 and 235.7 eV, respectively, for the flash evaporated  $MoO_3$  films. The Mo-3d core-level spectrum of as-deposited  $MoO_3$  films prepared at room temperature ( $T_{sub} = RT$ , Fig. 4(a)) is broader and having lesser intensity than those of the as-deposited films prepared at higher substrate temperatures (i.e.,  $T_{sub} = 100^\circ C$  and  $200^\circ C$ —Fig. 4(b) and (c)) and annealed films ( $T_{anne} = 300^\circ C$ —Fig. 4(d)). It is reasonable to support that this broadening is due to the difference in electrical environment around Mo site and also the amorphous nature of the films. The amorphous nature of RT deposited  $MoO_3$  films is also evident from the structural

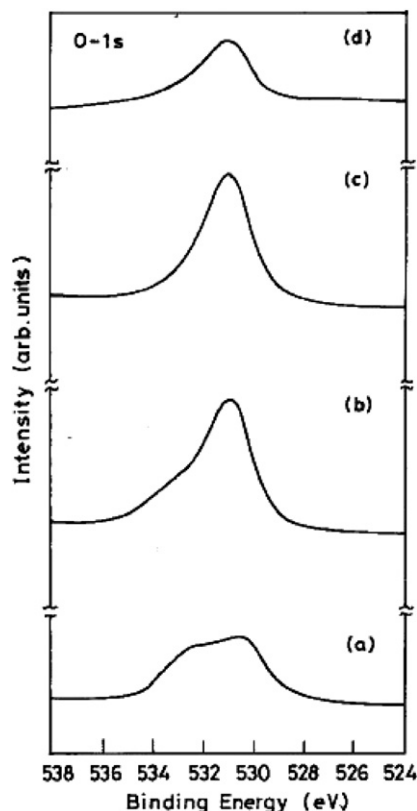


Fig. 5. XPS core-level spectra of oxygen (O-1s) for MoO<sub>3</sub> films (a)  $T_{\text{sub}} = \text{RT}$ , (b)  $T_{\text{sub}} = 100\text{ }^{\circ}\text{C}$ , (c)  $T_{\text{sub}} = 200\text{ }^{\circ}\text{C}$  and (d)  $T_{\text{anne}} = 300\text{ }^{\circ}\text{C}$ .

characterization. When we increased the substrate temperature (i.e.,  $T_{\text{sub}} = 100\text{ }^{\circ}\text{C}$ —Fig. 4(b) and  $200\text{ }^{\circ}\text{C}$ —Fig. 4(c)) as well as the annealing temperature ( $T_{\text{sub}} = \text{RT}$ ,  $T_{\text{anne}} = 300\text{ }^{\circ}\text{C}$ , Fig. 4(d)), we obtained the well resolved and sharper peaks, indicating an improvement in the film crystallinity, which can also be correlated with our X-ray diffraction studies [8,9].

Fig. 5(a)–(d) shows the characteristic core-level peak position for the O-1s state of MoO<sub>3</sub> films. From the spectra the O-1s binding energy was found to be 530.83 eV, independent of the temperatures, which is quite close to the binding energy of the reported literature [4]. The areas of the Mo (3d) and O (1s) peaks were used to determine the concentrations of molybdenum and oxygen on the film surface. The evaluated concentration of O and Mo and their

corresponding core-level binding energies are summarized in Table 1. The concentration of Mo and O in room temperature prepared MoO<sub>3</sub> films was found to be equal to 14.2% and 85.8%, respectively. But the concentration of Mo and O was evaluated as 28% and 72% from the films prepared at higher temperature of  $200\text{ }^{\circ}\text{C}$ . Thus, it enumerated the optimized MoO<sub>3</sub> films prepared in the present work was formed to their stoichiometric formulation. Table 1 clearly shows the decrease in concentration of oxygen with increasing substrate and annealing temperatures, which reconciled the formation of oxygen ion vacancies in the films. This also causes slight decrease in optical transmission and energy band gap of the films. Fig. 6(a)–(b) also evident the decrease in optical energy band gap ( $E_g$ ) of MoO<sub>3</sub> films with increasing substrate and annealing temperatures, obtained from optical studies by UV–Vis–NIR spectrophotometer [8,9]. These observations of our earlier work are providing the supportive evidence and correlating well with the results obtained in the present work.

### 3.2. (a) Electrochemical analysis

The electrochromic properties of MoO<sub>3</sub> films were studied by intercalating/deintercalating H<sup>+</sup> ions using three electrode electrochemical cell containing H<sub>2</sub>SO<sub>4</sub> (0.05 M and 0.1 M) electrolyte solutions. The optimized MoO<sub>3</sub> films on FTO substrates were used as the working electrodes. The platinum wire and saturated calomel electrode (SCE) were used instead of the counter and reference electrodes, respectively. The process of ion intercalation and deintercalation was noted during the cycling of different sweep rates such as 100, 200 and 300 mV/s. The currents resulting from these scan rates were measured during both the ion intercalation and deintercalation processes denoted as cathodic spike current ( $i_{\text{pc}}$ ) and anodic peak current ( $i_{\text{pa}}$ ), respectively. During the intercalation of these ions i.e., in the negative potential of the scan, the films have changed their colors into dark blue and return to their original color in the positive potential i.e., while the deintercalation of ions. All the samples were stable throughout the scan rates and also upto  $1 \times 10^3$  cycles of coloration/bleaching. Hence, these observations of reaction mechanism and also the coloration ↔ bleaching behaviour of MoO<sub>3</sub> films confirmed their perfect electrochemical proper-

Table 1  
X-ray photoelectron spectroscopic data of MoO<sub>3</sub> films with respect to different substrate and annealing temperatures

Sample	Binding energy ( $E_b$ ) (eV)			Atomic concentration (%)	
	Mo-3d <sub>5/2</sub>	Mo-3d <sub>3/2</sub>	O-1s	Mo	O
MoO <sub>3</sub> /glass/ $T_{\text{sub}} \text{ RT}$	232.32	235.44	530.83	14.2	85.8
MoO <sub>3</sub> /glass/ $T_{\text{sub}} 100\text{ }^{\circ}\text{C}$	232.32	235.44	530.83	25.1	74.9
MoO <sub>3</sub> /glass/ $T_{\text{sub}} 200\text{ }^{\circ}\text{C}$	232.32	235.44	530.83	28.0	72.0
MoO <sub>3</sub> /glass/ $T_{\text{anne}} 300\text{ }^{\circ}\text{C}$	232.32	235.44	530.83	25.9	74.1
Literatures	232.67 <sup>a</sup>	235.86 <sup>a</sup>	530.61 <sup>a</sup>	–	–
	232.30 <sup>b</sup>	235.70 <sup>b</sup>	530.00 <sup>b</sup>	–	–

<sup>a</sup> Ref. [4].

<sup>b</sup> Ref. [12].

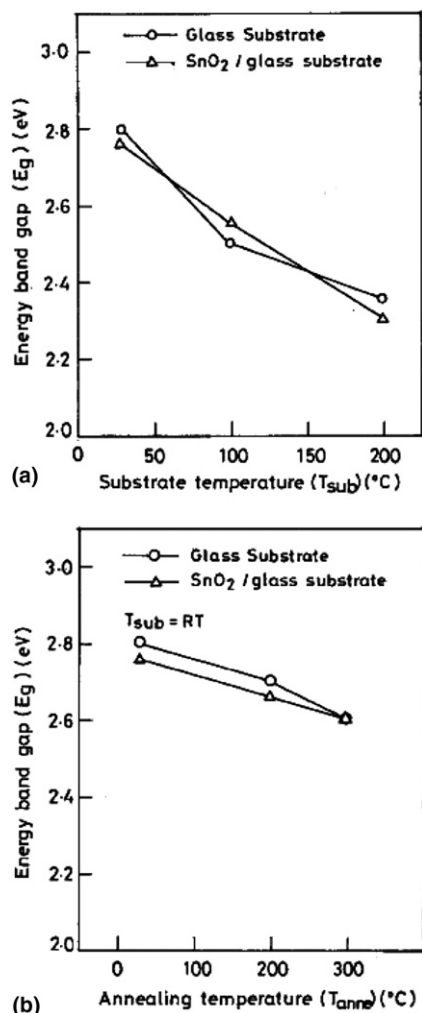


Fig. 6. Variation of energy band gap,  $E_g$  of MoO<sub>3</sub> films, (a) with respect to substrate temperatures and (b) with respect to annealing temperatures.

ties and also the suitability in low cost electrochromic devices.

The cyclic voltammograms of MoO<sub>3</sub> films deposited on FTO substrates at different temperatures like  $T_{sub} = 30$  °C (RT),  $T_{sub} = 100$  °C,  $T_{sub} = 200$  °C,  $T_{anne} = 200$  °C and  $T_{anne} = 300$  °C, cycled in 0.05 M H<sub>2</sub>SO<sub>4</sub> electrolyte solution are shown in Fig. 7(a)–(e), respectively. The CV diagrams of MoO<sub>3</sub> films recorded in 0.1 M H<sub>2</sub>SO<sub>4</sub> electrolyte are shown in Fig. 8(a)–(e). These voltammograms were recorded in the potential range between  $-1.2$  and  $+1.2$  V<sub>SCE</sub>. The voltammograms clearly show all the samples are having better reversibility and reproducibility in their electrochemical analysis.

The diffusion coefficients of ions during intercalation and deintercalation can be calculated by employing the Randles–Sergeik equation [1]

$$i_p = 2.72 \times 10^5 n^{\frac{3}{2}} D^{\frac{1}{2}} C_0 v^{\frac{1}{2}}, \quad (2)$$

where  $D$  is the diffusion coefficient of M<sup>+</sup> ions (in the present case M<sup>+</sup> = H<sup>+</sup>),  $v$  is the scan rate,  $n$  is the number of electrons and it is assumed to be 1,  $C_0$  is the concentration of ac-

tive ions in the electrolyte solution and  $i_p$  is the peak current (both anodic  $i_{pa}$  and cathodic  $i_{pc}$ ). The extracted electrochemical parameters from these CV diagrams are given in Tables 2 and 3. The calculated diffusion coefficients of H<sup>+</sup> ions ( $D_{H^+}$ ) in 0.05 M H<sub>2</sub>SO<sub>4</sub> solution, are  $7.78 \times 10^{-12}$ – $1.65 \times 10^{-7}$  cm<sup>2</sup>/s. The  $D$  value has been evaluated for the range of  $2.67 \times 10^{-13}$ – $1.04 \times 10^{-7}$  cm<sup>2</sup>/s in 0.1 M H<sub>2</sub>SO<sub>4</sub> electrolyte solutions. From electrochromic characterization of MoO<sub>3</sub> films using the three electrode electrochemical cell, it is observed that the performance of anodic peak and cathodic spike current improved with the increasing scan rate values. The electrochemical stability and reproducibility of the films are good throughout the experiments. The electrochemical process is still active for higher temperature prepared films. But the magnitude of both  $i_{pa}$  and  $i_{pc}$  and also the performance of electrochromic nature are slightly less in the films produced at higher substrate and annealing temperatures than the room temperature prepared films.

### 3.3. (b) Studies on electrochromic device (ECD) cells

The extensive electrochemical performance of the films was studied in ECD cells. The schematic inset of ECD cells is shown in Fig. 9. Typical electrochromic devices consist of the following: the working electrode (WE) was the FTO bearing the electrochromic film, while the counter electrode (CE) was the other FTO plate. Platinum wire acted as a pseudo-reference electrode (RE) and was placed in equidistant between the CE and WE. For coloring, an external voltage is applied. Electrons are injected into the electrochromic layer from the FTO and cations, i.e., M<sup>+</sup> from the electrolyte. The reverse happens for the bleaching process. The electron-transfer reaction occurs within thin films of electrochromic oxide (MoO<sub>3</sub>) sandwiched between a transparent electrode of fluorine doped tin oxide (FTO) coated glass substrates and an electrolyte, which allows for ready conduction of the M<sup>+</sup> ions (H<sup>+</sup> or K<sup>+</sup> or Li<sup>+</sup>) needed for charge balance in solid-solution electrodes; this arrangement with protons for M<sup>+</sup>, can be expressed as

FTO / EC / electrolyte / FTO

The simple and clear illustrations of the electrochromic devices are shown schematically in the literatures [14–16].

The change in optical transmittance of the colored and bleached films was studied by using Hitachi-3400 UV–Vis–NIR spectrophotometer. In order to observe the changes in optical transmittance spectra of colored and bleached films as a function of substrate and annealing temperatures, the optical density ( $OD_\lambda$ ) was evaluated. The coloration efficiency (CE) is also one of the very important parameters in electrochromic devices to identify the electrochemical performance of the films.

Optical density (OD) of the films was calculated from transmittance spectrophotometry [17] by

$$OD_\lambda = \log \left( \frac{T_{0\lambda}}{T_{x\lambda}} \right), \quad (3)$$

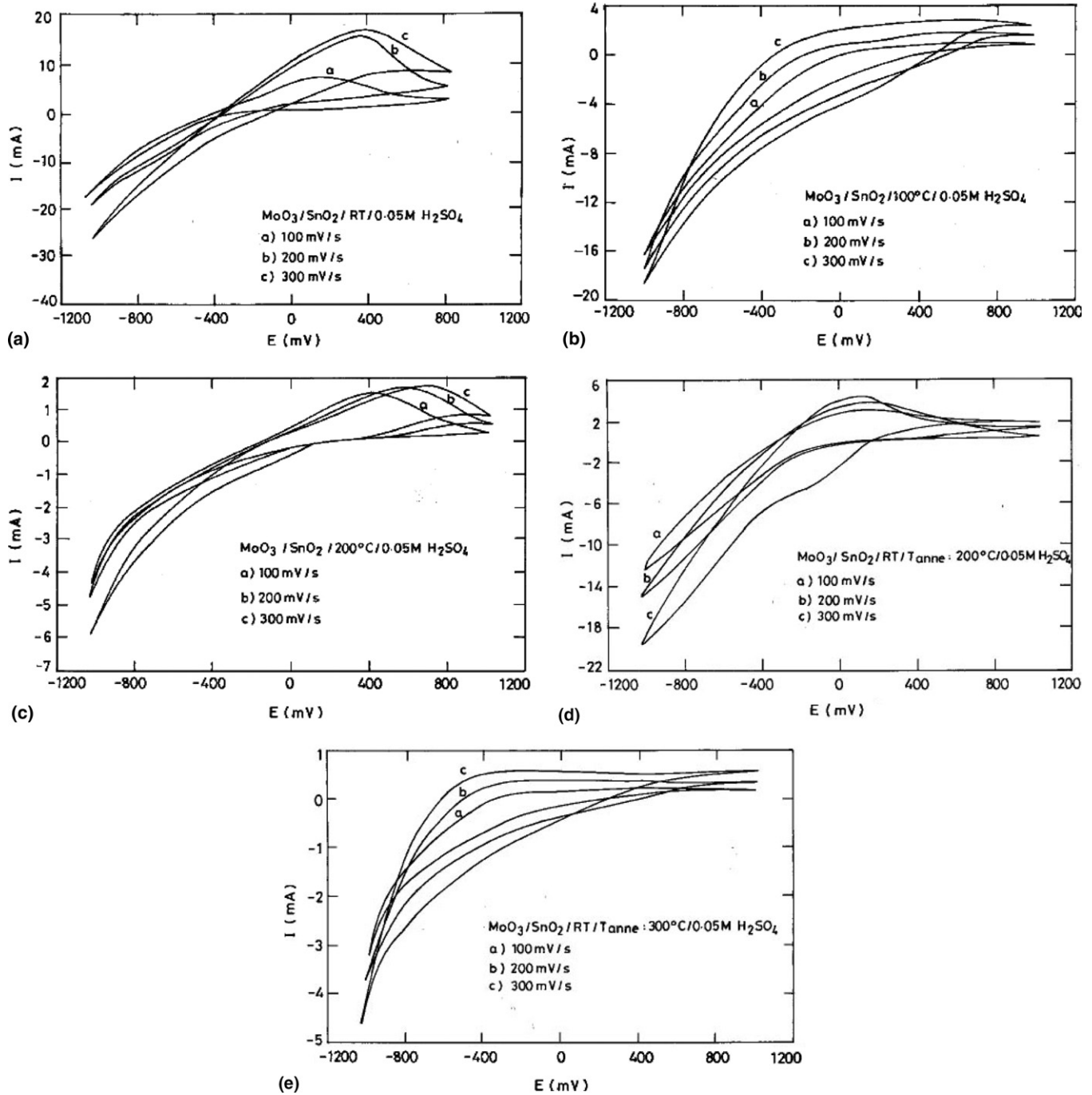


Fig. 7. Cyclic voltammograms of  $\text{MoO}_3$  films prepared at different conditions, cycled in 0.05 M  $\text{H}_2\text{SO}_4$  electrolyte solutions, (a)  $T_{\text{sub}} = \text{RT}$ , (b)  $T_{\text{sub}} = 100^\circ\text{C}$ , (c)  $T_{\text{sub}} = 200^\circ\text{C}$ , (d)  $T_{\text{anne}} = 200^\circ\text{C}$  and (e)  $T_{\text{anne}} = 300^\circ\text{C}$ .

where  $T_{0\lambda}$  is the reference transmittance and  $T_{x\lambda}$  is the measured transmittance. We choose the reference transmittance as the bleached state then the expression for optical density is [18]

$$OD_\lambda = \log \left( \frac{T_{b\lambda}}{T_{c\lambda}} \right), \quad (4)$$

where  $T_{b\lambda}$  is the bleached transmittance at wavelength  $\lambda$  and  $T_{c\lambda}$  is the colored transmittance at wavelength  $\lambda$ .

The coloration efficiency (CE) is defined by

$$CE = \frac{OD}{Q_{\text{in}}}, \quad (5)$$

where OD is the optical density given by Eq. (4) and  $Q_{\text{in}}$  ( $\text{mC}/\text{cm}^2$ ) is the charge injected during the coloration cycle.

The optimized  $\text{MoO}_3$  films deposited on fluorine doped tin oxide coated glass substrates by electron beam evaporation technique have been employed as working electrodes in the electrochromic devices. The electrochromic performance of  $\text{MoO}_3$  films prepared at conditioned  $T_{\text{sub}} = \text{RT}$ ,

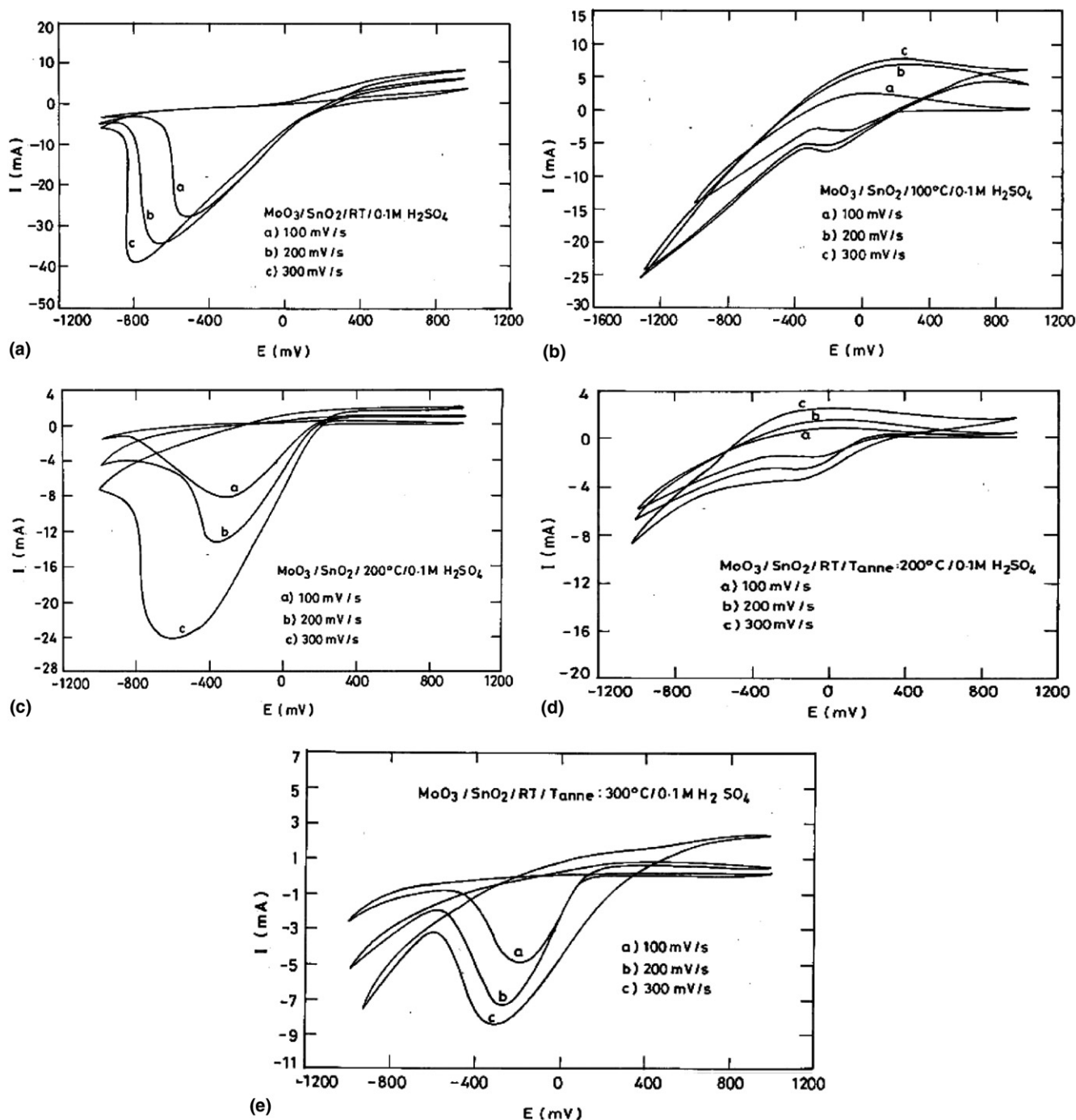


Fig. 8. Cyclic voltammograms of  $\text{MoO}_3$  films prepared at different conditions, cycled in 0.1 M  $\text{H}_2\text{SO}_4$  electrolyte solutions, (a)  $T_{\text{sub}} = \text{RT}$ , (b)  $T_{\text{sub}} = 100^\circ\text{C}$ , (c)  $T_{\text{sub}} = 200^\circ\text{C}$ , (d)  $T_{\text{anne}} = 200^\circ\text{C}$  and (e)  $T_{\text{anne}} = 300^\circ\text{C}$ .

$T_{\text{sub}} = 200^\circ\text{C}$  and  $T_{\text{anne}} = 300^\circ\text{C}$ , was studied in the ECD cells. The optical transparency of these films was studied for their coloration and bleaching process cycled in 0.1 M  $\text{H}_2\text{SO}_4$  electrolyte solutions. To color the  $\text{MoO}_3$  films, an external potential was applied across the platinum electrode and the transparent FTO electrode on which the films were deposited, in an electrolyte solution. By applying the electric field, electrons from the liquid electrolyte are simultaneously injected into the  $\text{MoO}_3$  films, and the films turns to blue in color.

The optical transmittance spectra of  $\text{MoO}_3$  films prepared at  $T_{\text{sub}} = \text{RT}$ ,  $200^\circ\text{C}$  and  $T_{\text{anne}} = 300^\circ\text{C}$ , cycled in 0.1 M  $\text{H}_2\text{SO}_4$  electrolyte solution are shown in the Fig. 10(a)–(c), respectively. From the colored and bleached states, it is observed that all the films show good electrochromic coloration. The higher optical modulation was observed in the visible range of the spectra; whereas the lower optical modulation was observed in the infrared range, which enumerated the suitability of these films in electrochromic device and smart window applications.

Table 2  
Electrochemical parameters of MoO<sub>3</sub> films associated with intercalation/deintercalation of H<sup>+</sup> ions cycled in 0.05 M H<sub>2</sub>SO<sub>4</sub> electrolyte solution

Sample	Scan rate, <i>v</i> (mV/s)	Cathodic spike current, <i>i</i> <sub>pc</sub> (mA)	Anodic peak current, <i>i</i> <sub>pa</sub> (mA)	Diffusion coefficient, <i>D</i> (cm <sup>2</sup> /s)	
				For <i>i</i> <sub>pc</sub>	For <i>i</i> <sub>pa</sub>
MoO <sub>3</sub> /RT	100	17.5	6.8	1.65 × 10 <sup>-7</sup>	2.50 × 10 <sup>-8</sup>
	200	20.0	14.9	1.08 × 10 <sup>-7</sup>	6.00 × 10 <sup>-8</sup>
	300	27.7	16.8	1.38 × 10 <sup>-7</sup>	5.08 × 10 <sup>-8</sup>
MoO <sub>3</sub> /100 °C	100	16.4	0.87	1.45 × 10 <sup>-7</sup>	4.09 × 10 <sup>-10</sup>
	200	17.8	1.75	8.56 × 10 <sup>-8</sup>	8.27 × 10 <sup>-10</sup>
	300	18.8	2.75	6.36 × 10 <sup>-8</sup>	1.36 × 10 <sup>-9</sup>
MoO <sub>3</sub> /200 °C	100	4.4	1.4	1.04 × 10 <sup>-8</sup>	1.16 × 10 <sup>-9</sup>
	200	4.8	1.6	6.22 × 10 <sup>-9</sup>	7.00 × 10 <sup>-10</sup>
	300	6.0	1.7	6.48 × 10 <sup>-9</sup>	5.71 × 10 <sup>-10</sup>
MoO <sub>3</sub> /RT/ <i>T</i> <sub>anne</sub> : 200 °C	100	12.3	2.8	8.27 × 10 <sup>-8</sup>	4.39 × 10 <sup>-9</sup>
	200	15.1	3.5	6.19 × 10 <sup>-8</sup>	3.44 × 10 <sup>-9</sup>
	300	19.4	4.4	6.83 × 10 <sup>-8</sup>	3.61 × 10 <sup>-9</sup>
MoO <sub>3</sub> /RT/ <i>T</i> <sub>anne</sub> : 300 °C	100	3.1	0.1	5.50 × 10 <sup>-9</sup>	7.78 × 10 <sup>-12</sup>
	200	3.8	0.3	3.92 × 10 <sup>-9</sup>	3.70 × 10 <sup>-11</sup>
	300	4.6	0.5	3.94 × 10 <sup>-9</sup>	5.65 × 10 <sup>-11</sup>

Table 3  
Electrochemical parameters of MoO<sub>3</sub> films associated with intercalation and deintercalation of H<sup>+</sup> ions cycled in 0.1 M H<sub>2</sub>SO<sub>4</sub> electrolyte solution

Sample	Scan rate, <i>v</i> (mV/s)	Cathodic spike current, <i>i</i> <sub>pc</sub> (mA)	Anodic peak current, <i>i</i> <sub>pa</sub> (mA)	Diffusion coefficient, <i>D</i> (cm <sup>2</sup> /s)	
				For <i>i</i> <sub>pc</sub>	For <i>i</i> <sub>pa</sub>
MoO <sub>3</sub> /RT	100	27.8	4.20	1.04 × 10 <sup>-7</sup>	2.38 × 10 <sup>-9</sup>
	200	34.2	7.10	7.90 × 10 <sup>-8</sup>	3.40 × 10 <sup>-9</sup>
	300	38.9	8.50	6.81 × 10 <sup>-8</sup>	3.25 × 10 <sup>-9</sup>
MoO <sub>3</sub> /100 °C	100	14.3	2.27	2.76 × 10 <sup>-8</sup>	6.96 × 10 <sup>-10</sup>
	200	24.5	6.80	4.05 × 10 <sup>-8</sup>	3.12 × 10 <sup>-10</sup>
	300	25.9	7.70	3.02 × 10 <sup>-8</sup>	2.67 × 10 <sup>-13</sup>
MoO <sub>3</sub> /200 °C	100	8.0	0.33	8.65 × 10 <sup>-9</sup>	1.47 × 10 <sup>-11</sup>
	200	13.5	0.83	1.23 × 10 <sup>-8</sup>	4.65 × 10 <sup>-11</sup>
	300	24.0	1.66	2.59 × 10 <sup>-8</sup>	1.24 × 10 <sup>-10</sup>
MoO <sub>3</sub> /RT/ <i>T</i> <sub>anne</sub> : 200 °C	100	6.1	0.87	5.02 × 10 <sup>-9</sup>	1.02 × 10 <sup>-10</sup>
	200	7.0	1.60	3.31 × 10 <sup>-9</sup>	1.73 × 10 <sup>-10</sup>
	300	9.3	2.50	3.89 × 10 <sup>-9</sup>	2.81 × 10 <sup>-10</sup>
MoO <sub>3</sub> /RT/ <i>T</i> <sub>anne</sub> : 300 °C	100	5.0	0.18	3.37 × 10 <sup>-9</sup>	4.37 × 10 <sup>-12</sup>
	200	7.2	0.45	3.57 × 10 <sup>-9</sup>	1.36 × 10 <sup>-11</sup>
	300	8.4	2.10	3.17 × 10 <sup>-9</sup>	1.98 × 10 <sup>-10</sup>

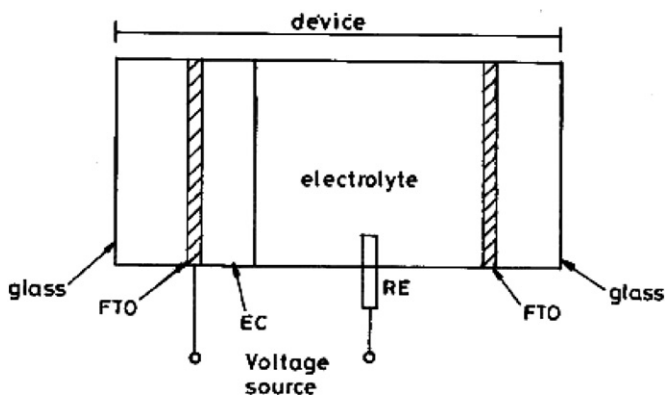


Fig. 9. Schematic inset of electrochromic device (ECD) cells.

However, the films produced at 200 °C exhibit a lower transmission range in the visible region compared to the film deposited at  $T_{\text{sub}} = \text{RT}$  (30 °C). The annealed films ( $T_{\text{anne}} = 300$  °C) also show the lower range in their visible region. The optical density (OD) and coloration efficiency (CE) of the films were calculated at the wavelength range of about 633 nm and 1033 nm. Table 4 clearly illustrates the magnitudes of optical density and coloration efficiency associated with the Fig. 10. The corresponding graphical representation of the evaluated optical density and coloration efficiency of MoO<sub>3</sub> films is shown in Fig. 11. The evaluated optical density of MoO<sub>3</sub> films lies in the range between 0.26 and 0.56, whereas the coloration efficiency is 44 and 70 cm<sup>2</sup>/C. The films produced at lower substrate

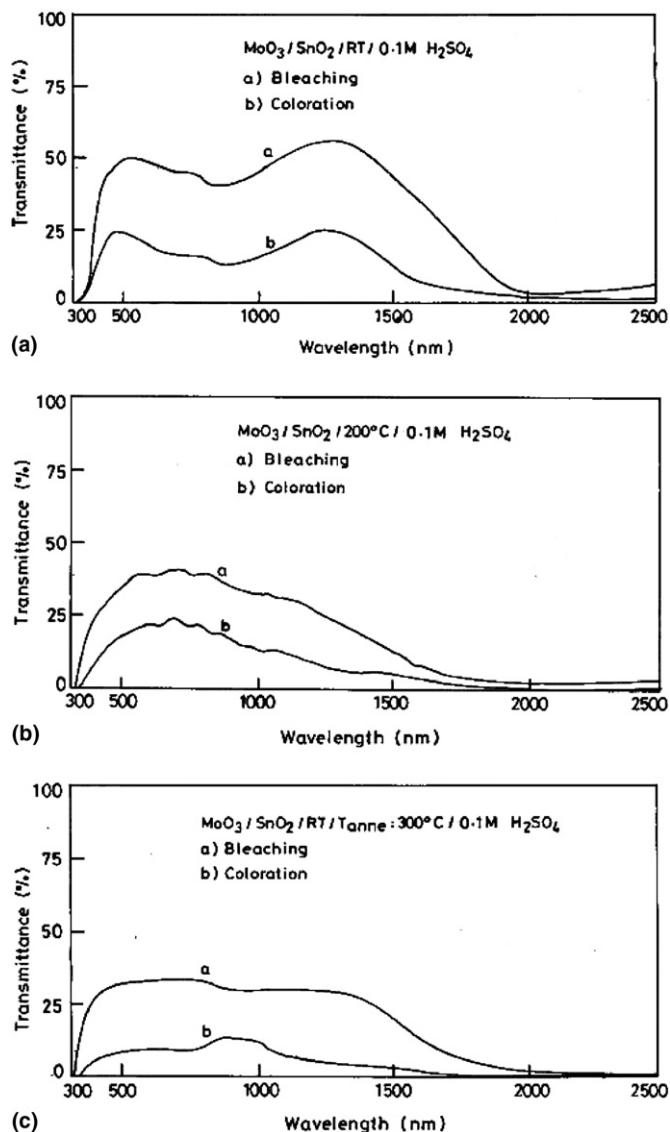


Fig. 10. Optical transmittance spectra of MoO<sub>3</sub> films in ECD cells, cycled in 0.1 M H<sub>2</sub>SO<sub>4</sub> electrolyte solutions, (a)  $T_{\text{sub}} = \text{RT}$ , (b)  $T_{\text{sub}} = 200\text{ }^\circ\text{C}$  and (c)  $T_{\text{anne}} = 300\text{ }^\circ\text{C}$ .

temperature (i.e.,  $T_{\text{sub}} = \text{RT}$ ) have higher coloration efficiency in the visible region ( $\lambda \sim 633\text{ nm}$ ) than those obtained for the films produced at higher substrate temperature ( $T_{\text{sub}} = 200\text{ }^\circ\text{C}$ ) and annealing temperature ( $T_{\text{anne}} = 300\text{ }^\circ\text{C}$ ). But, in the case of IR range ( $\lambda \sim 1033\text{ nm}$ ); the CE of MoO<sub>3</sub> films deposited at 200 °C is higher than the room temperature prepared films.

However, the literatures also infer the lesser performance of electrochromic behaviour for MoO<sub>3</sub> films in its

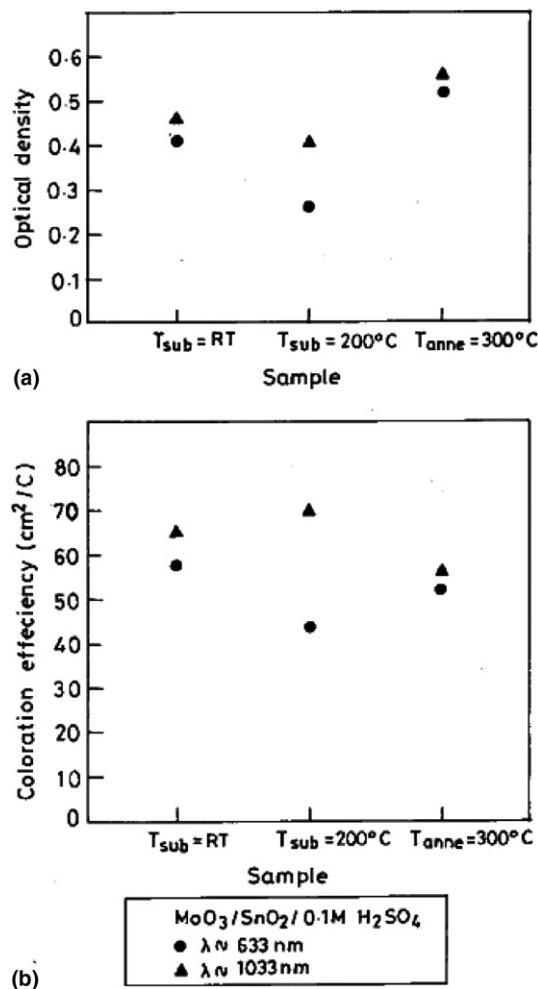


Fig. 11. Variation of the electrochromic device parameters of MoO<sub>3</sub> films with respect to substrate and annealing temperatures in 0.1 M H<sub>2</sub>SO<sub>4</sub> electrolyte solutions, (a) optical density (OD), (b) coloration efficiency (CE).

crystalline nature. Julien et al. [19,20] studied the Li<sup>+</sup> ion intercalation into MoO<sub>3</sub> films made by flash evaporation and their results showed  $D_{\text{Li}^+}$  lies between  $10^{-12}$  and  $5 \times 10^{-12}\text{ cm}^2/\text{s}$ . Patil and Patil [21] reported the H<sup>+</sup> ion intercalation from H<sub>2</sub>SO<sub>4</sub> electrolyte solution into mixed MoO<sub>3</sub>–WO<sub>3</sub> films and their results show the  $D_{\text{H}^+}$  lies in the range of  $10^{-10}\text{ cm}^2/\text{s}$ . Guylaine Laperriere et al. [11] reported the coloration efficiency of MoO<sub>3</sub> films decreases with increasing annealing temperature. Guerfi et al. [4] reported the coloration efficiency between 650 and 820 nm is equal to 41 cm<sup>2</sup>/C that can be linked to the moderate deep blue color of the heated film at 260 °C. Kitao

Table 4  
Evaluated ECD cell parameters of MoO<sub>3</sub> films in 0.1 M H<sub>2</sub>SO<sub>4</sub> electrolyte solution

Sample	Optical density (OD)		Coloration efficiency (CE) (cm <sup>2</sup> /C)	
	at $\lambda \sim 633\text{ nm}$	at $\lambda \sim 1033\text{ nm}$	at $\lambda \sim 633\text{ nm}$	at $\lambda \sim 1033\text{ nm}$
MoO <sub>3</sub> /RT	0.41	0.46	58	65
MoO <sub>3</sub> /200 °C	0.26	0.41	44	70
MoO <sub>3</sub> /RT/ $T_{\text{anne}}$ : 300 °C	0.52	0.56	52	56

and Yamada [22] evaluated the coloration efficiency of MoO<sub>3</sub> films at different wavelength ranges and their magnitudes are about 40–80 cm<sup>2</sup>/C.

Also, the observed cyclic voltammograms in the present work are similar in shape to those of previously reported for MoO<sub>3</sub> [4,10,11,21]. Thus, the obtained performance of electrochromic nature of MoO<sub>3</sub> films in ECD cells is supported with earlier studies, which reveals the suitability of MoO<sub>3</sub> films in electrochromic device applications.

#### 4. Conclusions

Based on the requirements of device-based electrochromic films, in the present investigation, thin films of molybdenum (MoO<sub>3</sub>) have been prepared onto microscopic glass and fluorine doped tin oxide coated glass substrates by electron beam evaporation technique. The X-ray photoelectron spectroscopic analysis confirms the material purity and compositional stoichiometry of MoO<sub>3</sub> films. The observed binding energies for Mo-3d<sub>5/2</sub> and Mo-3d<sub>3/2</sub> core-levels are well agreed with reported literatures, which reveal the presence of six-valence molybdenum (Mo<sup>6+</sup>) in the films.

It is observed from the electrochemical analysis and ECD cell characterization, the performance of the films is high in the room temperature prepared films. The reason is that the lower substrate temperature minimizes the extent of crystallinity and favours the amorphous nature of the films. Hence, the amorphous films enhance the coloration efficiency. When the films turned to crystalline, the extent of coloration would be slight because:

- (i) it is difficult for the counter ions to enter the crystallites;
- (ii) difference in morphology: it is harder and therefore slower for a counter ion to move through a more dense film.

Hence it reveals that the coloration efficiency and electrochemical performance of the films strongly depend on the preparative conditions, substrate temperature and annealing temperatures.

In conclusion, our results indicate the MoO<sub>3</sub> films prepared in the present work have good electrochromism and a better reversibility in their electrochromic coloration–decoloration process. Also it could be observed that the electron beam evaporation technique can produce device quality electrochromic oxide films, which are useful for electrochromic device applications. Hence our result presented in this paper support the idea of using the MoO<sub>3</sub> films as the good aesthetic materials in electrochromic windows.

#### Acknowledgements

The authors would like to acknowledge Dr. R. Gopalakrishnan, Crystal Research Laboratory, Department of Physics, Anna University, Chennai, India and Dr. P.M.S. Monk, Department of Chemistry and Materials, Manchester Metropolitan University, Manchester M1 5GD, for their fruitful scientific discussions in this part of the work. Authors also grateful to Dr. P. Manisankar, Department of Chemistry, Periyar University, Salem, India, for his help in this work. One of the authors R.S. gratefully acknowledge the Council of Scientific and Industrial Research (CSIR, New Delhi), Govt. of India, for awarding the Senior Research Fellowship.

#### References

- [1] C.G. Granqvist, Handbook of Inorganic Electrochromic Materials, Elsevier, Amsterdam, 1995.
- [2] P.M.S. Monk, R.J. Mortimer, D.R. Rosseinsky, Electrochromism: Fundamentals and Applications, VCH, Weinheim, 1995.
- [3] R.E. Thorne, Phys. Today 49 (1996) 42.
- [4] A. Guerfi, R.W. Paynter, Le H. Dao, J. Electrochem. Soc. 142 (1995) 3457.
- [5] M. Ferroni, V. Guidi, G. Martinelli, P. Nelli, M. Sacerdoti, G. Sberveglieri, Thin Solid Films 307 (1997) 148.
- [6] K. Gesheva, A. Szekeres, T. Ivanova, Sol. Energ. Mater. Sol. Cells 76 (2003) 563.
- [7] A. Bouzidi, N. Benramdane, H. Tabet-Derraz, C. Mathieu, B. Khelifa, R. Desfeux, Mater. Sci. Eng. B 97 (2003) 5.
- [8] R. Sivakumar, M. Jayachandran, C. Sanjeeviraja, Surf. Eng. 20 (2004) 385.
- [9] R. Sivakumar, R. Gopalakrishnan, M. Jayachandran, C. Sanjeeviraja, Curr. Appl. Phys., in press, doi:10.1016/j.cap.2005.10.001.
- [10] S. Liu, Q. Zhang, E. Wang, S. Dong, Electrochem. Commun. 1 (1999) 365.
- [11] G. Laperriere, M.-A. Lavoie, D. Belanger, J. Electrochem. Soc. 143 (1996) 3109.
- [12] C. Julien, A. Khelifa, O.M. Hussain, G.A. Nazri, J. Cryst. Growth 156 (1995) 235.
- [13] D. Belanger, G. Laperriere, Chem. Mater. 2 (1990) 484.
- [14] A. Hauch, A. Georg, S. Baumgartner, U. Opara Krasovec, B. Orel, Electrochim. Acta 46 (2001) 2131.
- [15] P.M.S. Monk, J.A. Duffy, M.D. Ingram, Electrochim. Acta 43 (1998) 2349.
- [16] M.D. Ingram, J.A. Duffy, P.M.S. Monk, J. Electroanal. Chem. 380 (1995) 77.
- [17] C.M. Lampert, V.-V. Truong, J. Nagai, Characterization Parameters and Test Methods for Electrochromic Device in Glazing Applications, International Energy Agency, Task X-C, Glazing Materials, Interim Working Document LBL – 29632.43e.
- [18] J. Wang, J.M. Bell, Sol. Energ. Mater. Sol. Cells 43 (1996) 377.
- [19] C. Julien, L. El-Farh, M. Balkanski, O.M. Hussain, G.A. Nazri, Appl. Surf. Sci. 65–66 (1993) 325.
- [20] C. Julien, O.M. Hussain, L. El-Farh, M. Balkanski, Solid State Ionics 53–56 (1992) 400.
- [21] P.R. Patil, P.S. Patil, Thin Solid Films 382 (2001) 13.
- [22] M. Kitao, S. Yamada, in: B.V.R. Chowdari, S. Radhakrishna (Eds.), Solid State Ionic Devices, World Scientific, Singapore, 1998, p. 359.